



Ni tracer diffusion in CoCrFeNi and CoCrFeMnNi high entropy alloys

M. Vaidya ^{a, b, *}, S. Trubel ^a, B.S. Murty ^b, G. Wilde ^a, S.V. Divinski ^{a, **}

^a Institute of Materials Physics, University of Münster, Wilhelm-Klemm-Str. 10, 48149, Münster, Germany

^b Department of Metallurgical & Materials Engineering, Indian Institute of Technology Madras, Chennai, 600036, India

ARTICLE INFO

Article history:

Received 9 May 2016

Received in revised form

22 July 2016

Accepted 22 July 2016

Available online 25 July 2016

Keywords:

High-entropy alloys

Tracer diffusion

Correlation factor

Point defects

ABSTRACT

High entropy alloys (HEAs) are multicomponent alloys in equiatomic or nearly equiatomic composition. Anticipated sluggish atomic diffusion is reported to be one of the core effects in HEAs which is presumably responsible for their many unique properties. For the first time, in the present study, tracer (Ni) diffusion in CoCrFeNi and CoCrFeMnNi alloys is measured by the radiotracer technique in the temperature range of 1073–1373 K using the ^{63}Ni isotope. Chemically homogeneous alloys of equiatomic composition were prepared by a vacuum arc melting route. The microstructure and phase stability of the alloys in the given temperature range is confirmed by differential thermal analysis and X-ray diffraction.

Ni diffusion in both CoCrFeNi and CoCrFeMnNi alloys is found to follow Arrhenius behavior. When plotted against the homologous temperature, a tendency to a successive slow down of the tracer diffusion rate with an increased number of components in equiatomic alloys is unambiguously established. Both the entropy term as well as the energy barriers is revealed to contribute to this trend. The current results indicate that diffusion in HEAs cannot a priori be considered as sluggish.

© 2016 Elsevier B.V. All rights reserved.

1. Introduction

High entropy alloys (HEAs) are multicomponent alloys, developed based on a novel design concept of multi-principal elements, containing constituents in equiatomic or nearly equiatomic proportions [1]. Yeh et al. [2] stated that such alloys tend to form simple solid solutions instead of complex phases or compounds due to their high configurational entropy of mixing (ΔS_{mix}). However, some recent studies have debated the dominance of configurational entropy in determining phase stability in high entropy alloys. Zhang et al. [3] have affirmed that a high mixing entropy state does not always have the lowest Gibbs energy and complex phases may precipitate out in HEAs on prolonged annealing. Ma and co-workers have argued that solid solutions present in HEA need not be entropy stabilized [4] and ab-initio calculations for CoCrFeMnNi indicate that vibrational, electronic and magnetic entropies are equally important as the configurational one [5]. Schuh et al. [6] have demonstrated phase decomposition in severely deformed CoCrFeMnNi alloy at 450 °C, which further hints

that high ΔS_{mix} does not guarantee the phase stability and often the single phase observed in HEAs is a high temperature phase whose transformation is possibly kinetically constrained. Pickering and Jones [7] have questioned the deemed significance of the proposed core effects (high entropy, severe lattice distortion, cocktail effect and sluggish diffusion) in HEAs.

Slow diffusion kinetics in HEAs is believed to be responsible for their unique features like excellent thermal stability, decelerated grain growth and formation of nano-precipitates [1]. Praveen et al. [8] have observed an excellent resistance to grain coarsening in nanocrystalline CoCrFeNi alloy and have partly attributed to slower atomic transport in HEAs. Lee et al. [9] have discussed the role of sluggish diffusion on enhanced creep resistance in nanocrystalline CoCrFeMnNi. In recent years, increased number of HEAs have been investigated for high temperature mechanical properties [10,11], creep strength [9,12–14], oxidation resistance [15–17] and coating applications [18]. Thus, understanding their diffusion kinetics is very important and of high relevance. Furthermore, reliable diffusion data are required as a key input for rigorous phase prediction using, e.g. the CALPHAD approach [3].

Nevertheless, only three experimental studies have been published so far limiting the present knowledge exclusively to interdiffusion data in HEAs. Tsai et al. [19] have determined the interdiffusion coefficients using a pseudo-binary approach [20] for a composition CoCrFeMn_{0.5}Ni which corresponded to the

* Corresponding author. Institute of Materials Physics, University of Münster, Wilhelm-Klemm-Str. 10, 48149, Münster, Germany.

** Corresponding author.

E-mail addresses: mmayur007@gmail.com (M. Vaidya), [\(S.V. Divinski\).](mailto:divin@wwu.de)

Kirkendall plane in that experiment. They have proposed that the derived values are approximately equal to the intrinsic and tracer diffusivities of the equiatomic CoCrFeMnNi alloy, arguing that the involved thermodynamic factor is about unity. The observed lower diffusion rates were attributed to a higher normalized activation enthalpy (Q/T_m , where Q is the activation enthalpy and T_m is the melting point of the alloy) of diffusion in HEAs as compared to pure metals and the corresponding binary and ternary alloys. However the authors emphasized that, in addition to the approximation of the thermodynamic factor by just unity, the analysis was performed by neglecting the off-diagonal terms in the Onsager matrix [19], too.

Very recently, Kulkarni and Chauhan [21] determined the diffusion matrix in CoCrFeNi at 1000 °C from an interdiffusion experiment and have argued that the role of diffusional interactions is very important in HEAs. This fact questions the estimates in Ref. [19] and calls for direct *tracer* measurements. Very recently, Dabrowska et al. [22] have studied interdiffusion in non-equiatomic AlCoCrFeNi alloys and further reported sluggish diffusion in HEAs. They also highlighted the importance of crystallographic parameters in determining the diffusion behavior in HEAs, rather than simply attributing it to varied chemical environments. Beke and Erdélyi [23] have re-analyzed the data presented in Ref. [19] and indicated the role of the correlation factors towards sluggish diffusion in HEAs.

We therefore summarize that only interdiffusion has been investigated in HEAs so far and presently the fundamental tracer diffusion data are completely missing for HEAs, although the term 'sluggish diffusion' is often used in case of HEAs. Furthermore, short-circuit, especially grain boundary diffusion, which contributes definitely to the enhanced creep properties is totally unknown, too.

We have to emphasize that the tracer diffusion method is superior with respect to the interdiffusion one, since it is the most direct way for measuring self-diffusion of an element in any alloy of a given composition and it corresponds to the presence of purely entropic driving forces [24]. The tracer concentrations are kept very small (typically at a ppm level) which allows diffusion investigations in a chemically homogeneous solid. It also ensures that diffusion of a tracer atom is not influenced by any other tracer and gives reliable self-diffusion coefficients of the constituent elements. Complications arising due to the presence of concentration gradients or cross-terms (like in interdiffusion [24]) play no role here. Accurate concentration profiles are obtained using nuclear counting facilities of a high sensitivity [25] and the tracer diffusion coefficients can directly be compared to the results of computer simulation in order to validate an anticipated diffusion mechanism.

In the present work, we report the first direct and assumption-free experimental results on the tracer diffusion of Ni in equiatomic CoCrFeNi and CoCrFeMnNi high entropy alloys. The primary objective of the present study is to establish whether an increase in the configurational entropy slows down diffusion in HEAs indeed. For example, CoCrFeMnNi has a significantly lower melting point (at least by 80 K) than all alloys which were compared in Ref. [19]. Therefore, a natural question is raised whether the mixing entropy decelerates diffusion at a given absolute temperature irrespective of a presumably increased vacancy concentration in the material due to depression of the melting point.

In order to address the above issue, we have chosen to study Ni tracer diffusivity in both CoCrFeNi and CoCrFeMnNi HEAs, which have significantly different melting points and ΔS_{mix} , see Table 1. These alloys were shown [26] to possess an FCC structure with the lattice parameter being close to that of Ni. The CoCrFeMnNi alloy does not decompose at temperatures higher than 1000 K [27] and CoCrFeNi preserves its single phase FCC state after annealing at

Table 1

Melting points (T_m) and Configurational entropy (ΔS_{mix}) of various FCC alloys. R is the universal gas constant.

Alloy	Melting point, T_m (K)	Reference for T_m	$\Delta S_{\text{mix}}/R$
Ni	1728	[38]	0
Fe-45.3Ni	1723	[38]	0.69
Fe-15Cr-20Ni	1731	[19]	0.89
CoCrFeNi	1717	Present work	1.39
FeCoCrMn _{0.5} Ni	1607	[19]	1.59
CoCrFeMnNi	1607	Present work	1.61

753 K for two weeks [28]. Therefore, Ni is our first choice to understand tracer diffusion in these HEAs at temperatures where a single phase FCC matrix is unambiguously preserved, and diffusion of other constituent elements is a subject of our on-going work.

2. Experimental details

Solid pieces (99.99 wt % purity) of Co, Cr, Fe, Mn and Ni were taken in equiatomic proportions and arc melted to form CoCrFeNi and CoCrFeMnNi alloys. The melting was carried out in a highly purified Ar atmosphere, preceded by an evacuation to 10^{-5} mbar pressure. Each alloy was re-melted 4–5 times to improve the chemical homogeneity. The buttons were further homogenized at 1473 K for 50 h. X-ray diffraction (XRD) (Cu-K α radiation) and scanning electron microscope (SEM) equipped with electron back-scattered diffraction (EBSD) and energy dispersive spectroscopy (EDS) were used to determine the phase structure, grain size and composition of the alloys. To ascertain the phase stability of alloys over the temperature-time domain of diffusion measurements, two separate annealing treatments for each alloy were carried out. The disc samples were sealed in quartz tubes with purified (5 N) Ar atmosphere and annealed in a SiC furnace at 1073 K and 1373 K for 31 days and 3 days respectively, followed by water quenching to retain the high temperature phase. The melting points of the alloys were determined using Differential Thermal Analysis (DTA). The heat flux measurements up to 1873 K were carried out in a Labsys TG-DSC under highly purified Ar applying a linear heating rate of 20 K/min.

The radioactive isotope ^{63}Ni (68 keV β -decays, half-life of 100 years) was used in the form of a highly diluted acidic solution. It was deposited on polished disc-shaped samples of 8 mm in diameter and 1 mm thickness. Subsequently, diffusion annealing treatments were carried out in sealed quartz tubes under purified (5 N) Ar atmosphere at the temperatures 1073 K, 1173 K and 1373 K for different times. After annealing, the diameter of the samples was reduced by approximately 1 mm to remove the contaminant effects of surface and lateral diffusion. The penetration profiles were determined by the serial sectioning technique using a high-precision grinding machine. The intensity of β -radiation of ^{63}Ni decays (which is proportional to the ^{63}Ni concentration in a section) was measured using a liquid-scintillation counter TRI CARB 2910TR. The counting time was chosen to keep the statistical uncertainty of the activity determination below 2%. The initial (few) sections (up to 1 μm in total depth) may represent artifacts induced by the calibration procedure of a sample for parallel grinding and/or by very fine surface scales and, therefore, are not included in the penetration profiles.

3. Results and discussion

The phase stability of the material at the temperatures and for the times of the intended diffusion annealing treatments is a key factor for a straightforward and reliable determination of the

diffusion parameters. Note that due to the use of radioactive tracers a post-diffusion characterization of the alloys is not feasible.

Therefore, the as processed (cast and homogenized) alloys were subjected to heat treatments at the lowest and highest temperatures and to the longest times of diffusion annealing employed in the present study (31 days at 1073 K and 3 days at 1373 K). The XRD results are presented in Fig. 1a and b for CoCrFeNi and CoCrFeMnNi, respectively. It is clear that both alloys possess a single-phase FCC structure which is retained during the annealing treatments. The peak shifts to lower θ -values for both CoCrFeNi and CoCrFeMnNi are partially due to calibration problems with measurements on different devices. In addition, relative intensity of the (200) peak is found to be higher than for the CoCrFeNi alloy annealed at 1073 K, which indicates a texture evolution. However, probable grain boundary motion and accompanied grain re-orientation, caused by texture, cannot affect the bulk tracer diffusion contribution, since tracer diffusion is isotropic in cubic lattices [24].

Orientation imaging microscopy using EBSD analysis was applied and Fig. 2 shows grain orientation maps and chemical maps obtained for as-processed (arc-melted and homogenized) CoCrFeNi and CoCrFeMnNi alloys. Grains are almost equiaxed, grain size exceeds 250 μm and dispersed Cr oxides (2–5 μm in size) are scarcely present. The EDX analysis confirms the homogeneity of the alloys, Fig. 2, and the equiatomic composition of CoCrFeNi as well as CoCrFeMnNi alloys, see Table 2.

For an accurate determination of the melting points, T_m , of the alloys, DTA analyses were performed. As indicated in Fig. 3, strong endothermic peaks corresponding to melting are observed for both CoCrFeNi and CoCrFeMnNi alloys at 1717 K and 1607 K, respectively. These values are used for the definition of the corresponding homologous temperatures, T/T_m , of the alloys. Here T is the absolute temperature. No further phase transformations are seen in the alloys over the entire temperature range, which in fact additionally indicates the stability of a single-phase structure of the alloys during the diffusion measurements. Generally, solidus, liquidus or peak temperatures can be used as melting points in numerical estimates of homologous temperatures below. It was proven that a given choice does not affect the main conclusions of the present paper.

The annealing conditions in the present study were found to correspond dominantly to a thin film geometry, for which the Gaussian solution of the bulk diffusion equation is appropriate,

$$C(x, t) = \frac{M}{\sqrt{\pi D t}} \exp\left(-\frac{x^2}{4 D t}\right). \quad (1)$$

Here $C(x, t)$ is the concentration at the depth x from the surface after the time t , D is the diffusion coefficient, and M is the initial

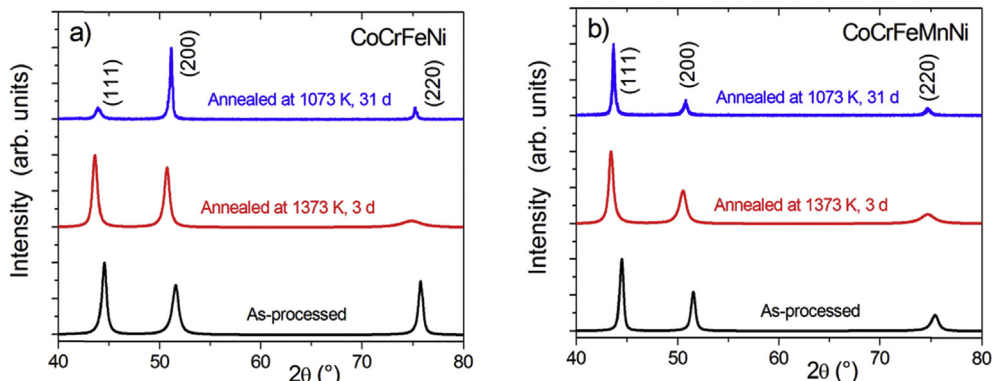


Fig. 1. X-ray diffractograms of as-processed and annealed CoCrFeNi (a) and CoCrFeMnNi (b) alloys. Only diffraction maxima corresponding to the FCC lattice are observed.

tracer amount. In some cases, especially at lower temperatures, the complementary error function solution [24] was found to be more appropriate.

A probable grain boundary diffusion contribution at these relatively high temperatures can be described in the framework of the so-called B-type kinetic regime after Harrison's classification [29] using Le Clair's functional form [30],

$$C(x, t) = C_0 \exp\left(-A \cdot x^{6/5}\right), \quad (2)$$

where C_0 and A are constants, see also [24,31].

The ^{63}Ni concentration profiles measured at 1173 K for CoCrFeNi and CoCrFeMnNi are given in Fig. 4 and this profile shape is observed at all other temperatures as well. A combination of Equations (1) And (2) has been used to fit the experimental data.

Two basic contributions can obviously be distinguished in Fig. 4. The first, near-surface branch of the profile corresponds certainly to a bulk tracer diffusion mechanism, and the tracer penetration profile is well linear in the coordinates of the logarithm of concentration against the depth squared. The alloy has sufficiently large grain size, d , consequently the ratio of grain boundary width to d is very small, which further substantiates that only lattice diffusion is dominant in the regions close to the surface [24].

The second branch of the profile in Fig. 4 could correspond to grain boundary diffusion as it seems to be linear against the depth to the 6/5 power, in accordance with Equation (2). The observance of pronounced grain boundary diffusion contribution at relatively high temperatures in our studies (especially at 1373 K in the FeCoCrMnNi alloy that corresponds to about $0.85T_m$ for this material) is not commonly observed in pure metals [31,32]. This needs a detailed investigation which is the subject of a separate study.

In the present paper, the diffusion data corresponding to the first branches of the concentration profiles are reported and they are presented in Fig. 5 for the two HEAs under investigation. The maximum penetration depth increases with increasing temperature and the diffusion coefficient, D , is determined as $D = -(1/4t)(\partial \ln C / \partial x^2)^{-1}$, where $\partial \ln C / \partial x^2$ is the slope of the penetration profile in the corresponding coordinates. In a single measurement, the estimated uncertainty of the determined tracer diffusion coefficients is below 20%.

By comparing diffusivities of different materials with the same structure, it was often found that the measured diffusion coefficients scale with the corresponding melting points of the compounds, T_m , for a detailed discussion see, e.g., Ref. [25]. Therefore, the derived diffusion coefficients from the concentration profiles are plotted as a function of inverse temperature, T^{-1} , and of inverse homologous temperature, T_m/T , in Fig. 6a and b,

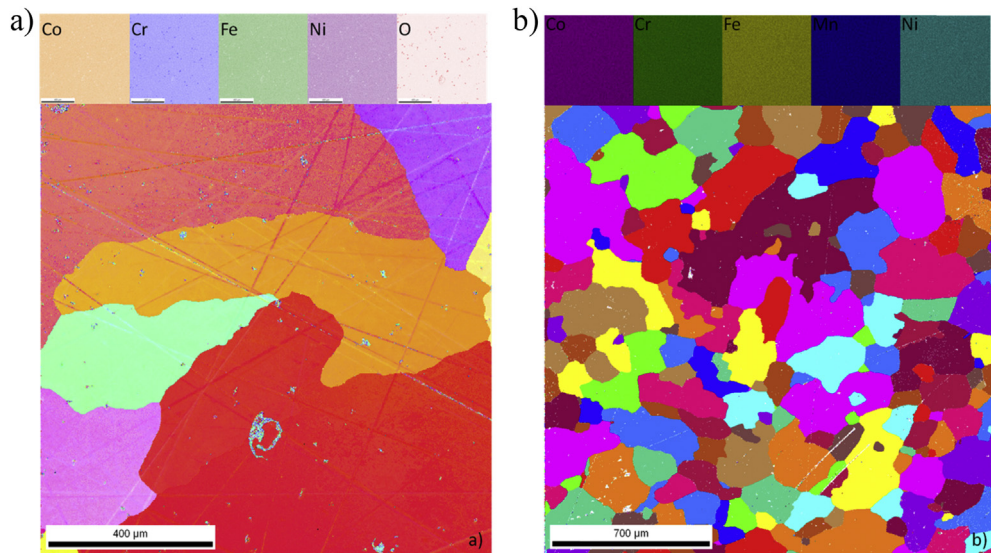


Fig. 2. Unique color mapping of grain orientations and the corresponding elemental maps obtained from SEM + EBSD analysis for a) CoCrFeNi b) CoCrFeMnNi. A uniform distribution of elements with a scarce presence of Cr oxide is observed.

Table 2

Composition of CoCrFeNi and CoCrFeMnNi alloys obtained from Energy Dispersive Spectroscopy (EDS) (Total no. of readings taken for each alloy, $n = 8$).

Elements	CoCrFeNi (atomic %)	CoCrFeMnNi (atomic %)
Co	24.5 ± 0.7	19.6 ± 0.6
Cr	25.9 ± 0.6	20.7 ± 0.5
Fe	24.7 ± 0.3	20.4 ± 0.6
Mn	—	19.3 ± 0.6
Ni	25.0 ± 0.6	20.0 ± 0.4

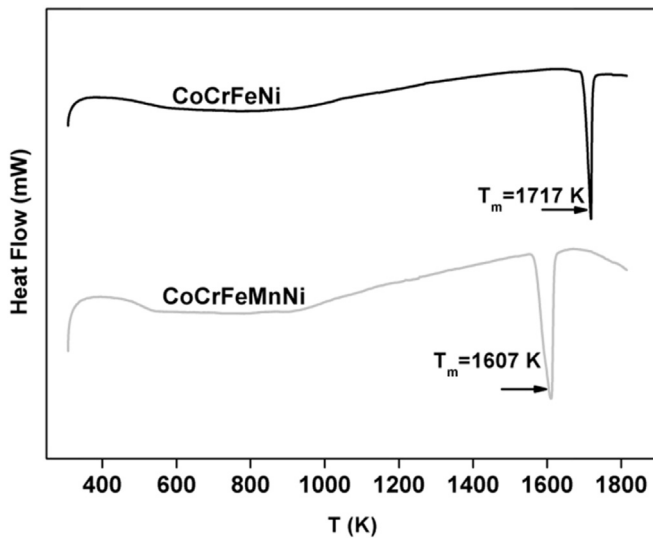


Fig. 3. Heat flow for the CoCrFeNi and CoCrFeMnNi alloys as measured by DTA with a constant heating rate of 20 K/min. The corresponding melting points are indicated.

respectively. A striking fact is that opposite diffusion trends are observed for these two cases. CoCrFeNi reveals a lower diffusivity than CoCrFeMnNi at all absolute temperatures, while it exhibits higher diffusion rates when diffusion is compared using the homologous temperature. The basic premise of sluggish diffusion in HEAs comes from the fact that an increased number of components

hinder the atomic movement due to varied chemical environments. The tendency reflected in Fig. 6a and b questions, however, the extent to which the configurational entropy slows down tracer diffusion. The ΔS_{mix} for the 5-component alloy is higher ($1.61R$) than for the 4-component alloy ($1.38R$), yet Ni tracer diffusion is slower in the 4-component alloy at a given absolute temperature. Thus, two salient features can be highlighted:

- If the inverse of homologous temperature, T_m/T , is used for comparison, there is a clear trend of diffusion retardation with an increased number of components in an alloy, i.e. with increased configurational entropy, cf. Fig. 6b.
- If the diffusion rates are compared at a given absolute temperature T , an increased number of the components in an alloy can result even in diffusion enhancement providing a depression of the melting point due to component addition.

Thus, the role of a configurational entropy term in diffusion is not straightforward. To further probe the influence of the enhanced mixing entropy on diffusion, a comparison with the literature data on diffusion in various FCC systems is given, Fig. 7. Fig. 7a documents the temperature dependence of Ni tracer diffusion in various FCC systems, while it is re-plotted against the inverse of homologous temperature in Fig. 7b. The original diffusion data are shown only for the temperature ranges reported in the corresponding papers. Fig. 7a suggests that Ni diffusion is not the slowest in CoCrFeMnNi even though it is characterized by the highest ΔS_{mix} value (Table 1). In addition, Fig. 7a also indicates that the tracer diffusivity of Ni in pure Ni is almost similar to binary Fe-Ni alloy, although the increase in configurational entropy is largest when we go from pure metal to binary alloy (Table 1). Perhaps, the reason why such observation has not been highlighted in literature until now is that up to 3 components, alloys are not classified as HEAs. However, let us analyze the figure more carefully and compare the four systems, i.e., pure Ni, binary Fe-45.3Ni, ternary Fe-15Cr-20Ni and quaternary CoCrFeNi (studied in this work). All these four FCC systems have very similar melting points (Table 1) and out of them, CoCrFeNi has the slowest Ni diffusion and the highest entropy of mixing. This fact reveals that an increase of the configurational entropy may decelerate the diffusion rate, but it is not, as

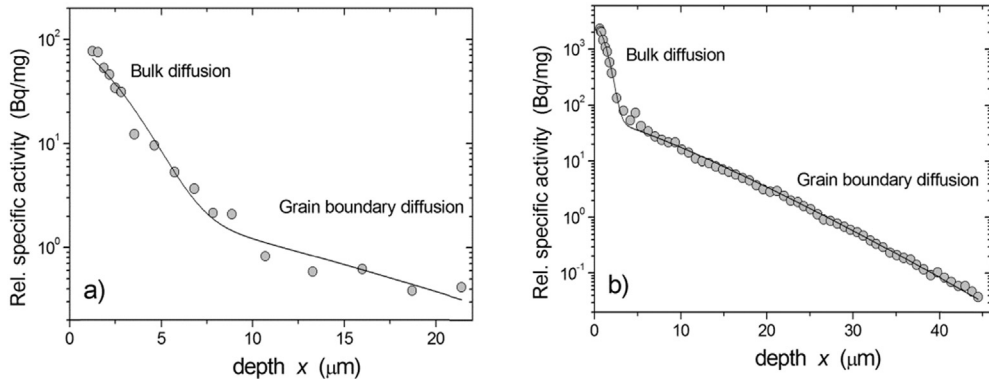


Fig. 4. Concentration profiles of ^{63}Ni tracer diffusion measured at 1173 K in the CoCrFeNi (a) and CoCrFeMnNi (b) alloys. The solid lines represent fits according to simultaneous bulk and grain boundary diffusion, see text.

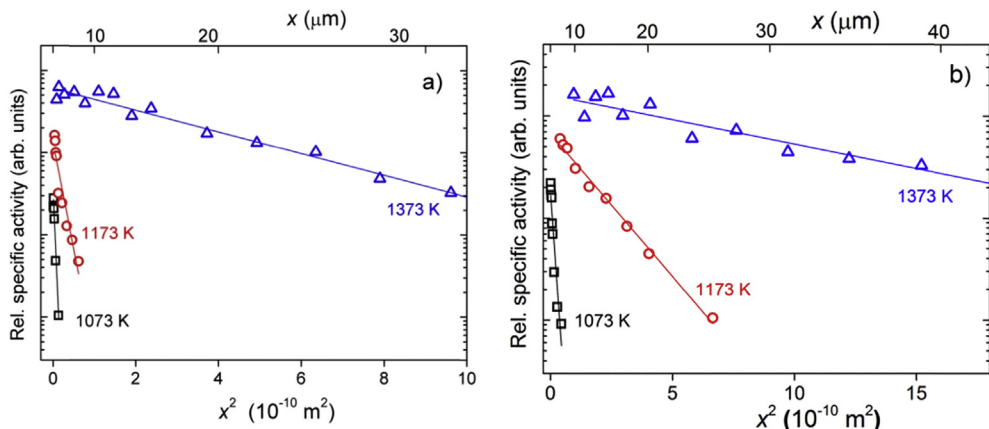


Fig. 5. The first branches (volume diffusion) of the concentration profiles measured for Ni diffusion in CoCrFeNi (a) and CoCrFeMnNi (b) alloys.

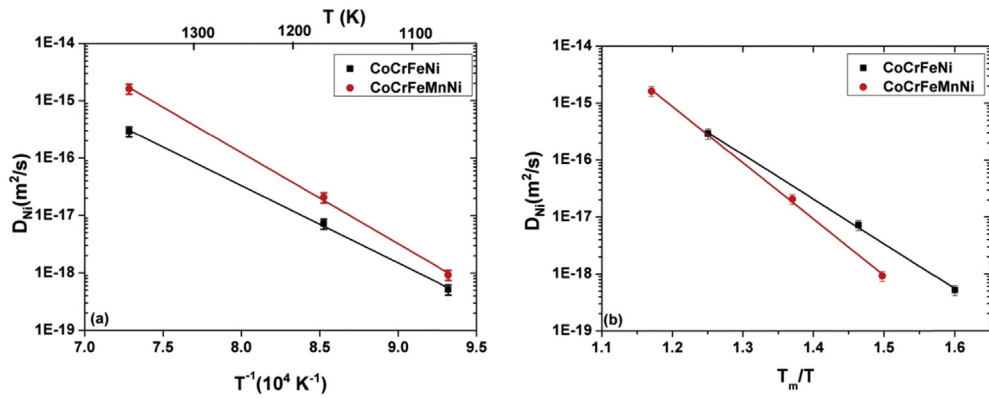


Fig. 6. Arrhenius diagrams for Ni diffusion in CoCrFeNi and CoCrFeMnNi alloys plotted using inverse absolute temperature (a) and inverse homologous temperature (b).

discussed above, the sole reason of ‘sluggish’ diffusion in the high entropy alloys. Fig. 7b ascertains that, when compared against the inverse homologous temperature, the decelerated diffusion kinetics does correlate with an increasing number of components in the alloys. Ni diffusion in CoCrFeMnNi at any homologous temperature is slower than in pure Ni by about two orders of magnitude.

The temperature dependence of the diffusivities is found to follow an Arrhenius behavior,

$$D = D_0 \exp\left(-\frac{Q}{RT}\right) \quad (3)$$

where D_0 is the pre-exponential factor, Q is the activation energy, and RT has its usual meaning. These parameters (i.e., D_0 and Q) for Ni diffusion in equiatomic HEAs and other FCC matrices are given in Table 3. It is evident from Equation (3) that the decreased diffusion rates can be caused by both, lower D_0 or higher Q values. The pre-factor D_0 is usually expressed as $D_0 = gfa^2\nu_0 \exp(\Delta S/R)$ [24], where

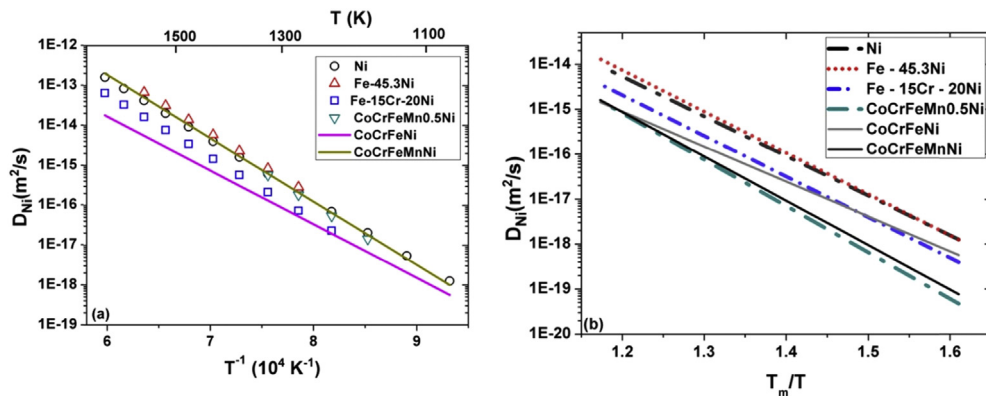


Fig. 7. Comparison of Ni tracer diffusivity in HEAs (the present work) and other FCC matrices: pure Ni [39], Fe-45.3Ni [40], Fe-15Cr-20Ni [41], and FeCoCrNiMn_{0.5} [19] when plotted against the inverse absolute temperature (a) and the inverse homologous temperature (b).

Table 3

Activation parameters for Ni diffusion in different FCC systems. R is the universal gas constant; T_m is the melting point in K.

Alloy	$D_0 (10^{-4} \text{ m}^2/\text{s})$	$Q (\text{kJ/mol})$	$Q^* = Q/RT_m$	Ref.
Ni	2.2	292	19.9	[39]
Fe-45.3Ni	8.04	303	21.2	[40]
Fe-15Cr-20Ni	1.50	300	20.8	[41]
FeCoCrNiMn _{0.5}	19.7	317	23.8	[19]
CoCrFeNi	$0.020^{+0.023}_{-0.011}$	257.8 ± 7.7	18.1	Present work
CoCrFeMnNi	$6.2^{+8.7}_{-3.6}$	303.9 ± 8.7	22.7	Present work

g is a geometric factor, f is the correlation factor, a is the lattice parameter, ν_0 is the attempt frequency, and ΔS is the diffusion entropy. Accepting an average lattice parameter of 0.355 nm, constant geometric and correlation factors (1 and 0.787, respectively) for the FCC lattice and taking ν_0 as the Debye frequency (10^{13} s^{-1}), ΔS has been calculated for these FCC systems and shown in Fig. 8. Obviously, CoCrFeNi reveals the lowest ΔS value that is reflected in decreased diffusion kinetics in this alloy. The diffusion entropy is the change of the entropy of lattice vibrations originating from a constrained movement of the diffusing atom through a saddle point configuration [33,34]. The low value of ΔS in CoCrFeNi can arise due to the presence of localized order. However, an exact determination of the diffusion entropy would require first principle calculations. The present experimental study thus appeals for a detailed consideration of the short range order in CoCrFeNi that

may significantly deviate from a random solution. Note that a further hint towards a (low-temperature) short range ordering of Cr atoms in the FeCoCrNi alloy was indicated [35].

Fig. 8 shows the normalized activation enthalpies, Q^* ($=Q/RT_m$), for different FCC systems, too, and it is evident that CoCrFeMnNi exhibits the highest Q^* value. This behavior can be rationalized by considering relative thermodynamic interaction of Ni with other constituent elements. Table 4 lists the mixing enthalpies of binary pairs constituting the equiatomic HEAs under investigation [36]. We calculate the average enthalpy of mixing of Ni with all other individual components ($\Delta H_{\text{avg}}^{\text{Ni}}$) in both 4 and 5 component alloys. $\Delta H_{\text{avg}}^{\text{Ni}}$ is -3.0 kJ/mol and -4.25 kJ/mol for CoCrFeNi and CoCrFeMnNi, respectively, which results from the fact that Ni-Mn has the strongest interaction among the different binaries (Table 4). Note that only pair interactions were included. Thus addition of Mn causes an increase of the $\Delta H_{\text{avg}}^{\text{Ni}}$ value and this fact correlates with an increase of the enthalpy of Ni tracer diffusion.

Mn, however, when alloyed to CoCrFeNi, may induce an opposite effect, too. Mn has a lower melting point than the other constituents and the melting temperature of the five-component alloy is lower than that of the quaternary one. (Note that a 'Vegard's law' of melting points was indeed shown to work reasonably well for binary intermetallics [37], although these reasonings are used here only in a qualitative way.) This implies that at any given absolute temperature, the equilibrium vacancy concentration is higher in CoCrFeMnNi, which will tend to increase the rate of substitutional

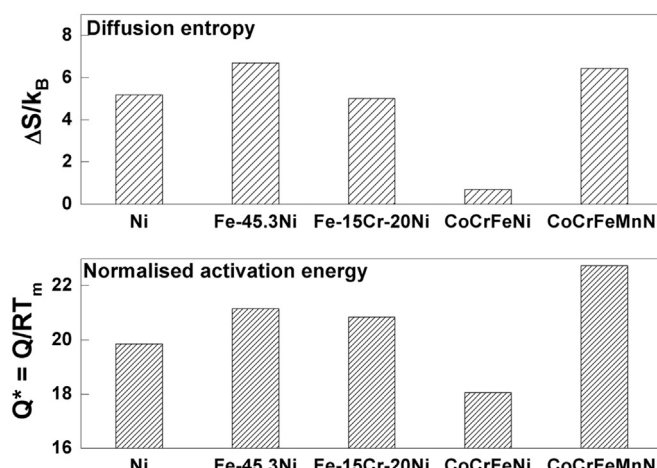


Fig. 8. Diffusion entropy ($\Delta S/R$) and normalized activation enthalpies ($Q^* = Q/RT_m$) for the FCC systems analyzed in the present work.

Table 4

Enthalpy of mixing for binary pairs in the multicomponent alloys [36].

Binary system	$\Delta H_{\text{mix}} (\text{kJ/mol})$	Binary system	$\Delta H_{\text{mix}} (\text{kJ/mol})$
Co-Cr	-4	Cr-Mn	2
Co-Fe	-1	Cr-Ni	-7
Co-Mn	-5	Fe-Mn	0
Co-Ni	0	Fe-Ni	-2
Cr-Fe	-1	Mn-Ni	-8

diffusion. The interplay of entropic and energetic effects can be seen in normalized Arrhenius plots for CoCrFeNi and CoCrFeMnNi, Fig. 6b. A cross-over homologous temperature, T^*/T_m , is observed, when the Arrhenius plot for quinary alloy is extrapolated to lower homologous temperatures, below which Ni diffuses in the five-component alloy with a lower rate than in the quaternary HEA due to an increased activation enthalpy. The increased activation energy of Ni diffusion in CoCrFeMnNi correlates with the more negative $\Delta H_{\text{avg}}^{\text{Ni}}$ value after Mn addition. At higher temperatures, above T^*/T_m , Ni diffusion is faster in CoCrFeMnNi with respect to that in CoCrFeNi due a significantly larger entropy factor.

We further conclude that the values derived from the interdiffusion experiments in Ref. [19] provide generally a reasonably fair estimate of tracer diffusion coefficient of Ni in the CoCrFeMnNi HEA within a factor of two. However, only after measurements of the diffusivities of other constituent elements the crucial assumption about the elimination of the off-diagonal terms in the Onsager matrix in Ref. [19] can be verified.

Diffusion in non-equiautomic Al-Co-Cr-Fe-Ni has been investigated by Dabrowa et al. [22]. A simple estimate shows that the configurational entropy of mixing for the alloys considered in Ref. [22] is approximately $1.5R$, which is not significantly different from ΔS_{mix} of equiatomic CoCrFeMnNi (Table 1). However, the activation enthalpy of Ni diffusion in non-equiautomic Al-Co-Cr-Fe-Ni was found [22] to be 227.1 kJ/mol, which is significantly lower than that for CoCrFeMnNi (303.9 kJ/mol as shown in Table 3). This fact further strengthens our claim that a high configurational entropy is not alone responsible for the increased activation barriers and consequently for the slower diffusion rates. The thermodynamic and topological properties of the elements added will certainly play a role in determining the extent and underlying mechanism of the diffusion process. We, therefore, accentuate that both energy barriers and frequency factors do contribute to the decreased diffusion rates in HEAs. For a proper accounting of all correlation effects, which may appear due to a variation of the local jump frequencies, the measurements of tracer diffusion coefficients of all constituents are required.

4. Conclusions

In the present work, tracer diffusion of an element, Ni, is measured for the first time in equiatomic HEAs. Two contributions to atomic transport kinetics are observed in the penetration profiles for both quaternary and quinary alloys, and the bulk diffusion coefficients are determined. It has been conclusively shown that while the configurational entropy may decelerate the diffusion kinetics, it must not be considered to be solely responsible for 'sluggish' diffusion in HEAs.

The temperature dependencies of Ni tracer diffusion in both HEAs follow an Arrhenius behavior. A low pre-exponential factor, D_0 , governs mainly the slow diffusion rates in CoCrFeNi, while the increased effective activation enthalpy is responsible for slower Ni diffusion in CoCrFeMnNi when analyzed as a function of the homologous temperature. A cross-over homologous temperature exists when the Arrhenius plots for Ni diffusion in CoCrFeNi and CoCrFeMnNi are compared, which arises probably due to two opposite effects of Mn addition on diffusion.

We conclude that diffusion in HEAs is not inevitably sluggish; in contrast, it can be even enhanced if the diffusion rates are compared at a given absolute temperature in the CoCrFeNi and CoCrFeMnNi alloys. Tracer diffusion in HEAs becomes relatively sluggish if considered at a given homologous temperature.

Acknowledgements

The authors wish to thank Dr. Prabhu for his help with the synthesis of alloys and Cand.-Phys. J. Kottke and C.Simon for a help with XRD and DTA measurements. M.V. is grateful to DAAD for a financial support of his research staying at the radiotracer laboratory, Institute of Materials Physics, University of Münster, Germany. Partial financial support of DFG, research project DI 1419/13-1, is also acknowledged.

References

- [1] B.S. Murty, J.W. Yeh, S. Ranganathan, *High Entropy Alloys*, Elsevier, London, 2014.
- [2] J.W. Yeh, S.K. Chen, S.J. Lin, J.Y. Gan, T.S. Chin, T.T. Shun, C.H. Tsau, S.Y. Chang, Nanostructured high-entropy alloys with multiple principal elements: novel alloy design concepts and outcomes, *Adv. Eng. Mater.* 6 (2004) 299–303.
- [3] F. Zhang, C. Zhang, S.L. Chen, J. Zhu, W.S. Cao, U.R. Kattner, An understanding of high entropy alloys from phase diagram calculations, *Calphad* 45 (2014) 1–10.
- [4] D. Ma, M. Yao, K.G. Pradeep, C.C. Tasan, H. Springer, D. Raabe, Phase stability of non-equiautomic CoCrFeMnNi high entropy alloys, *Acta Mater.* 98 (2015) 288–296.
- [5] D. Ma, B. Grabowski, F. Körmann, J. Neugebauer, D. Raabe, Ab initio thermodynamics of the CoCrFeMnNi high entropy alloy: importance of entropy contributions beyond the configurational one, *Acta Mater.* 100 (2015) 90–97.
- [6] B. Schuh, F. Mendez-Martin, B. Völker, E.P. George, H. Clemens, R. Pippan, A. Hohenwarter, Mechanical properties, microstructure and thermal stability of a nanocrystalline CoCrFeMnNi high-entropy alloy after severe plastic deformation, *Acta Mater.* 96 (2015) 258–268.
- [7] E.J. Pickering, N.G. Jones, High-entropy alloys: a critical assessment of their founding principles and future prospects, *Int. Mater. Rev.* (2016) 1–20.
- [8] S. Praveen, J. Basu, S. Kashyap, R.S. Kottada, Exceptional resistance to grain growth in nanocrystalline CoCrFeNi high entropy alloy at high homologous temperatures, *J. Alloys Compd.* 662 (2016) 361–367.
- [9] D.H. Lee, M.Y. Seok, Y. Zhao, I.C. Choi, J. He, Z. Lu, J.Y. Suh, U. Ramamurthy, M. Kawasaki, T.G. Langdon, J.I. Jang, Spherical nanoindentation creep behavior of nanocrystalline and coarse-grained CoCrFeMnNi high-entropy alloys, *Acta Mater.* 109 (2016) 314–322.
- [10] N.N. Guo, L. Wang, L.S. Luo, X.Z. Li, R.R. Chen, Y.Q. Su, J.J. Guo, H.Z. Fu, Hot deformation characteristics and dynamic recrystallization of the MoNbHfZrTi refractory high-entropy alloy, *Mater. Sci. Eng. A* 651 (2016) 698–707.
- [11] H. Chen, A. Kauffmann, B. Gorr, D. Schliephake, C. Seemüller, J.N. Wagner, H.-J. Christ, M. Heilmayer, Microstructure and mechanical properties at elevated temperatures of a new Al-containing refractory high-entropy alloy Nb-Mo-Cr-Ti-Al, *J. Alloys Compd.* 661 (2016) 206–215.
- [12] L. Zhang, P. Yu, H. Cheng, H. Zhang, H. Diao, Y. Shi, B. Chen, P. Chen, R. Feng, J. Bai, Q. Jing, M. Ma, P.K. Liaw, G. Li, R. Liu, Nanoindentation creep behavior of an Al₁₀.3CoCrFeNi high-entropy alloy, *Metall. Mater. Trans. A* (2016) 1–5.
- [13] Y. Ma, Y.H. Feng, T.T. Debela, G.J. Peng, T.H. Zhang, Nanoindentation study on the creep characteristics of high-entropy alloy films: fcc versus bcc structures, *Int. J. Refract. Met. H.* 54 (2016) 395–400.
- [14] T. Cao, J. Shang, J. Zhao, C. Cheng, R. Wang, H. Wang, The influence of Al elements on the structure and the creep behavior of Al_xCoCrFeNi high entropy alloys, *Mater. Lett.* 164 (2016) 344–347.
- [15] W. Kai, C.C. Li, F.P. Cheng, K.P. Chu, R.T. Huang, L.W. Tsay, J.J. Kai, The oxidation behavior of an equimolar FeCoNiCrMn high-entropy alloy at 950 °C in various oxygen-containing atmospheres, *Corros. Sci.* 108 (2016) 209–214.
- [16] G. Laplanche, U.F. Volkert, G. Eggeler, E.P. George, Oxidation behavior of the CrMnFeCoNi high-entropy alloy, *Oxid. Met.* 85 (2016) 629–645.
- [17] G.R. Holcomb, J. Tylczak, C. Carney, Oxidation of CoCrFeMnNi high entropy alloys, *JOM* 67 (2015) 2326–2339.
- [18] R.A. Shaginyan, N.A. Krapivka, S.A. Firstov, N.I. Danilenko, I.V. Serdyuk, Superhard vacuum coatings based on high-entropy alloys, *Powder Metall. Met. C* 54 (2016) 725–730.
- [19] K.Y. Tsai, M.H. Tsai, J.W. Yeh, Sluggish diffusion in Co–Cr–Fe–Mn–Ni high-entropy alloys, *Acta Mater.* 61 (2013) 4887–4897.
- [20] A. Paul, A pseudobinary approach to study interdiffusion and the Kirkendall effect in multicomponent systems, *Philos. Mag.* 93 (2013) 2297–2315.
- [21] K. Kulkarni, G.P.S. Chauhan, Investigations of quaternary interdiffusion in a constituent system of high entropy alloys, *AIP Adv.* 5 (2015) 097162.
- [22] J. Dabrowa, W. Kucza, G. Cieslak, T. Kulik, M. Danielewski, J.W. Yeh, Interdiffusion in the FCC-structured Al-Co-Cr-Fe-Ni high entropy alloys: experimental studies and numerical simulations, *J. Alloys Compd.* 674 (2016) 455–462.
- [23] D.L. Beke, G. Erdélyi, On the diffusion in high-entropy alloys, *Mater. Lett.* 164 (2016) 111–113.
- [24] A. Paul, T. Laurila, V. Vuorinen, S. Divinski, *Thermodynamics, Diffusion and Kirkendall Effect in Solids*, Springer, Switzerland, 2014.
- [25] H. Mehrer, *Diffusion in Solids: Fundamentals, Methods, Materials, Diffusion-controlled Processes*, Springer, Berlin, 2007.
- [26] G.A. Salishchev, M.A. Tikhonovsky, D.G. Shaysultanov, N.D. Stepanov,

- A.V. Kuznetsov, I.V. Kolodiy, A.S. Tortika, O.N. Senkov, Effect of Mn and V on structure and mechanical properties of high-entropy alloys based on CoCrFeNi system, *J. Alloys Compd.* 591 (2014) 11–21.
- [27] A. Gali, E.P. George, Tensile properties of high-and medium-entropy alloys, *Intermetallics* 39 (2013) 74–78.
- [28] M.S. Lucas, G.B. Wilks, L. Mauger, J.A. Munoz, O.N. Senkov, E. Michel, J. Horwath, S.L. Semiatin, M.B. Stone, D.L. Abernathy, E. Karapetrova, *Appl. Phys. Lett.* 100 (2012) 251907.
- [29] L.G. Harrison, Influence of dislocations on diffusion kinetics in solids with particular reference to alkali halides, *Trans. Faraday Soc.* 57 (1961) 1191–1197.
- [30] A.D. Le Claire, The analysis of grain boundary diffusion measurements, *Br. J. Appl. Phys.* 14 (1963) 351–356.
- [31] I. Kaur, Y. Mishin, W. Gust, *Fundamentals of Grain and Interface Boundary Diffusion*, Wiley & Sons Ltd., Chichester, New York, 1995.
- [32] S.V. Divinski, B.S. Bokstein, Recent advances and unsolved problems of grain boundary diffusion, *Defect Diffus. Forum* 309 (2011) 1–8.
- [33] C. Wert, C. Zener, Interstitial atomic diffusion coefficients, *Phys. Rev.* 76 (1949) 1169.
- [34] G.H. Vineyard, Frequency factors and isotope effects in solid state rate processes, *J. Phys. Chem. Solids* 3 (1957) 121.
- [35] C. Niu, A.J. Zaddach, A.A. Oni, X. Sang, J.W. Hurt III, J.M. LeBeau, C.C. Koch, D.L. Irving, Spin-driven ordering of Cr in the equiatomic high entropy alloy NiFeCrCo, *Appl. Phys. Lett.* 106 (2015) 161906.
- [36] A. Takeuchi, A. Inoue, Classification of bulk metallic glasses by atomic size difference, heat of mixing and period of constituent elements and its application to characterization of the main alloying element, *Mater. Trans.* 46 (2005) 2817–2829.
- [37] J.R. Chelikowsky, K.E. Anderson, Melting point trends in intermetallic alloys, *J. Phys. Chem. Solids* 48 (1987) 197–205.
- [38] Volume 3, ASM Handbook, *Alloy Phase Diagrams*, ASM International, 1992.
- [39] M.B. Bronfin, G.S. Bulatov, I.A. Drugova, Self-diffusion of Ni in the intermetallic compound Ni₃Al and pure Ni, *Fiz. Met. Metalloved.* 40 (1975) 363–366.
- [40] B. Million, J. Růžičková, J. Velíšek, J. Vršetál, Diffusion processes in the Fe-Ni system, *Mater. Sci. Eng.* 50 (1981) 43–52.
- [41] S.J. Rothman, L.J. Nowicki, G.E. Murch, Self-diffusion in austenitic Fe-Cr-Ni alloys, *J. Phys. F. Met. Phys.* 10 (1980) 383–398.